

LITERATURE CITED

- Bird, R. B., "Viscous Heat Effects in Extrusion of Molten Plastics," *SPE J.*, **11**, 35 (1955).
- , W. E. Stewart and E. N. Lightfoot, *Transport Phenomena*, Wiley, New York (1960).
- Bird, R. B., R. C. Armstrong and O. Hassager, *Dynamics of Polymeric Liquids*, Vol. 1, Fluid Mechanics, Wiley, New York (1977).
- Brinkman, H. C., "Heat Effects in Capillary Flow," *Appl. Sci. Res.*, **A2**, 120 (1951).
- Brown, G. M., "Heat or Mass Transfer in a Fluid in Laminar Flow in a Circular or Flat Conduit," *AIChE J.*, **6**, 179 (1960).
- Churchill, R. V., *Fourier Series and Boundary Value Problems*, 2 ed., McGraw-Hill, New York (1963).
- Cox, H. W., and C. W. Macosko, "Viscous Dissipation in Die Flows," *AIChE J.*, **20**, 785 (1974).
- Dang, V. D., "Low Peclet Number Heat Transfer for Power Law Non-Newtonian Fluid with Heat Generation," *J. Appl. Polymer Sci.*, **23**, 3077 (1979).
- Galili, N., R. Takserman-Krozer and Z. Rigbi, "Heat and Pressure Effect in Viscous Flow Through a Pipe, I. General Formulation and Basic Solution," *Rheol. Acta*, **14**, 550 (1975a).
- , "Heat and Pressure Effect in Viscous Flow Through a Pipe, II. Analytical Solution for Non-Newtonian Flow," *ibid.*, 816 (1975b).
- Gavis, J., and R. L. Laurence, "Viscous Heating of a Power-Law Liquid in Plane Flow," *Ind. Eng. Chem. Fundamentals*, **7**, 525 (1968).
- Gee, R. E., and J. B. Lyon, "Nonisothermal Flow of Viscous Non-Newtonian Liquids," *Ind. Eng. Chem.*, **49**, 956 (1956).
- Hieber, C. A., "Thermal Effects in the Capillary Rheometer," *Rheol. Acta*, **16**, 553 (1977).
- Hildebrand, F. B., *Introduction to Numerical Analysis*, McGraw-Hill, New York (1974).
- Kwant, P. B., and Th. N. M. Van Ravenstein, "Non-isothermal Laminar Channel Flow," *Chem. Eng. Sci.*, **28**, 1935 (1973).
- Middleman, S., *The Flow of High Polymers*, Interscience, New York (1968).
- Novotny, E. J., and R. E. Eckert, "Direct Measurement of Hole Error for Viscoelastic Fluids in Flow Between Infinite Parallel Plates," *Trans. Soc. Rheol.*, **17**, 222 (1973).
- , "Rheological Properties of Viscoelastic Fluids from Continuous Flow Through a Channel Approximating Infinite Parallel Plates," *ibid.*, **18**, 1 (1974).
- Seifert, A., "Wärmeübergang bei der Strömung von Prandtl-Eyring-Flüssigkeiten durch ebene Spalte. Mit Berücks. d. Dissipation u. unsymmetr. therm. Randbedingn." Doctoral thesis, Technische Universität, Berlin (1969).
- Suckow, W. H., P. Hrycak and R. G. Griskey, "Heat Transfer to Polymer Solutions and Melts Flowing Between Parallel Plates," *Polymer Eng. Sci.*, **11**, 401 (1971).
- Sukanek, P. C., "Poiseuille Flow of a Power-Law Fluid with Viscous Heating," *Chem. Eng. Sci.*, **26**, 1775 (1971).
- Tien, C., "The Extension of Couette Flow Solution to the Non-Newtonian Fluid," *Can. J. Chem. Eng.*, **39**, 45 (1961).
- , "Laminar Heat Transfer of Power-Law Non-Newtonian Fluid—The Extension of Graetz-Nusselt Problem," *ibid.*, **40**, 130 (1962).
- Toor, H. L., "The Energy Equation for Viscous Flow: Effect of Expansion on Temperature Profiles," *Ind. Eng. Chem.*, **48**, 922 (1956).
- , "Heat Generation and Conduction in the Flow of a Viscous Compressible Liquid," *Trans. Soc. Rheol.*, **1**, 177 (1957).
- Turian, R. M., "Viscous Heating in the Cone and Plate Viscometer, III, Non-Newtonian Fluids with Temperature Dependent Viscosity and Thermal Conductivity," *Chem. Eng. Sci.*, **20**, 771 (1965).
- Vlachopoulos, J., and C. K. J. Keung, "Heat Transfer to a Power-Law Fluid Flowing Between Parallel Plates," *AIChE J.*, **18**, 1272 (1972).
- Winter, H. H., "Temperature Fields in Extruder Dies with Circular, Annular, or Slit Cross-Section," *Polymer Eng. Sci.*, **15**, 84 (1975).
- , "Viscous Dissipation in Shear Flows of Molten Polymers," *Adv. Heat Transfer*, **13**, 205 (1977).
- Wohl, M. H., "Designing for Non-Newtonian Fluids, Part 5, Dynamics of Flow Between Parallel Plates and in Noncircular Ducts," *Chem. Eng.*, **75**, 183 (May 6, 1968).

Manuscript received August 29, 1979; revision received January 17, and accepted January 25, 1980.

Heat Transfer from Two-Phase Boundary Layers on Isothermal Cylinder: Influence of Drop Trajectory

The influence of drop trajectories on boundary layer structure and heat transfer coefficient is determined for a binary spray flow over the upstream surface of an isothermal cylinder. Governing equations are solved for drop trajectories upstream of the cylinder, the laminar liquid boundary layer adjacent to the cylinder surface, and the outer laminar vapor boundary layer. Velocity, temperature, and mass concentration profiles throughout the double boundary layers are shown to depend on flow parameters involving drop size and velocity. The critical conditions for which the liquid film dries out are identified for a range of drop size and velocity, defining the transition from the liquid film to the dry wall flow regime. Theoretical results for heat transfer are shown to correlate existing experimental data.

CHRISTOPHER C. LU

and

JOHN W. HEYT

Department of Chemical Engineering
The University of Dayton
Dayton, Ohio 45469

SCOPE

The increase in surface heat transfer resulting from the addition of liquid drops to a gas stream may contribute a significant reduction in size and operating cost of a heat exchanger. The application can also be used for the emergency cooling system in a nuclear reactor where liquid drops can be sprayed directly across a heating surface. The objective of this

study is to identify the effect of drop trajectory on the boundary layer structure and on the local heat transfer coefficient for a binary spray flow perpendicular to an isothermal cylinder. Drops of a single-component liquid are dispersed uniformly throughout the binary gas, which is composed of the vapor of the liquid drops and a noncondensable component. Gas and liquid flows are retarded near the stationary cylinder surface, forming a boundary layer. Drops which impinge on the cylinder surface form a liquid film which enhances the wall heat transfer.

John W. Heyt is with General Electric Corporation, South Portland, Maine 04104.

0001-1541-80-3731-0762-\$00.95. © The American Institute of Chemical Engineers, 1980.

CONCLUSIONS AND SIGNIFICANCE

The governing flow parameters such as Reynolds number, liquid drop concentration, drop size and surface temperature will determine the flow regime which exists at the heating surface. At low wall temperature, drops collect at the wall and form a thin liquid layer on the surface, with an outer spray boundary layer formed above the liquid film. Increased convection and conduction in the liquid layer and evaporation from the film surface are primary reasons for the increase in wall heat transfer in this regime. As the wall temperature is increased, the liquid layer will completely dry out owing to evaporation, resulting in the transition to the dry wall flow regime. The critical values of the flow parameters for which this transition occurs are particularly important for the prediction of heat transfer, since the physical nature of the boundary layer is very different in each case. A different theory for prediction of wall heat transfer must be applied for each re-

gime. In the present study, the boundary layer structure for binary spray flow over an isothermal circular cylinder is determined for the case in which the influence of drop trajectory upstream of the cylinder is significant.

It is also found in the present study that both inertia and drag forces of the drop particles essentially influence the drop trajectory of the binary spray flow. For a large inertia force and a small drag force, the drop particles tend to form a straight trajectory. On the contrary, for a small inertia force and a large drag force, the drop particles tend to follow the streamlines of the gas flow and move around the cylinder surface. A significant increase in the heat transfer coefficient is obtained by increasing the inertia force. The experimental data for the heat transfer coefficient obtained by Hodgson et al. (1966) is correlated using the governing nondimensional parameters defined in this study.

Early experimental data on heat transfer augmentation using a spray were obtained for tube bundles used in atmospheric condensers by James (1937), Goodman (1938), Thomsen (1946) and Wile (1950) and used in evaporative heat exchangers by Elperin (1961). The average heat transfer coefficient for the tube bundle is shown to increase as liquid concentration in the spray increases. In general, use of these data is limited to equipment of the same type, size and operating conditions.

To identify basic mechanisms which govern spray flow and are independent of equipment size and type, data on a single tube in spray flow have been obtained by Acrivos et al. (1964), Smith (1966), Hodgson et al. (1966), Hoelscher (1965) and Takahara (1966) for the case of an isothermal cylinder wall. The addition of the liquid spray is shown to increase the average heat transfer coefficient by a factor as large as 40. Measurements of the local heat transfer coefficient as a function of angular position on the cylinder surface have shown values to decrease from the stagnation point on the upstream face. Relatively small variation has been observed on the downstream surface. Mednick and Colver (1969) observed increases in the wall heat transfer coefficient by a factor as large as 30 in experiments on a circular cylinder with constant wall heat flux. Thomas (1967) has also measured substantial increase in wall heat transfer for a spray cooled wedge. The increase in surface heat transfer by a factor as large as 40 resulting from the addition of liquid drops to a gas stream has stimulated recent interest in basic fluid mechanics and heat transfer in spray flows.

Theoretical work on spray flow over an isothermal circular cylinder by Acrivos et al. (1964) dealt with the limiting case of creeping and inviscid flow. In an integral analysis of the liquid layer by Smith (1966), evaporation at the film surface was included in calculations of temperature profiles and overall heat transfer. In an extended integral analysis including third-order velocity and temperature profiles, theory by Hodgson and Sunderland (1968) correlates wall heat transfer data by Hodgson et al. (1966) at large liquid concentration but underestimates the data at low liquid concentration. The effect on wall heat transfer of drop trajectory in the flow outside the boundary layer was included by Goldstein et al. (1967), and the region near the stagnation point was studied by Yeh and Yang (1967). Loss of mass from the liquid layer because of evaporation was studied by Heyt and Jain (1972), showing the effect on wall heat transfer and giving critical flow parameters for the transition from the liquid film to the dry wall regime. Analysis of the cylinder with constant heat flux has been developed by Heyt and Lu (1972).

Analysis has also been applied by Tifford (1964) and Goldstein et al. (1967) to heat transfer on a flat plate in spray flow and by Thomas (1967) to the spray cooled wedge. Analysis for the dry

wall regime has been developed by Heyt and Larsen (1971) and compared to experimental data for flow parallel to a flat plate.

This study was conducted to determine the effect of drop trajectory on the local heat transfer coefficient and flow regime transition in binary spray flow normal to an isothermal cylinder. Boundary layer equations are written for conservation of mass, momentum and energy throughout both the liquid layer next to the wall and the outer spray layer. Interface conditions between the two layers match the transfer of mass, momentum and energy between the layers. Solutions give the velocity, temperature and mass concentration through both layers and the liquid layer thickness. Wall heat transfer and shear stress are then evaluated. Results for drop trajectory are compared to results for the assumption of straight drop trajectory, and experimental data of Hodgson et al. (1966) are correlated using the governing nondimensional parameters defined in the present theory.

ANALYSIS

The spray flow geometry is shown in Figure 1, where X and Y are the coordinates for drop trajectories upstream of the cylinder, and x and y are coordinates used in the boundary layer analysis located tangential and normal to the cylinder surface, respectively. The symbol U_∞^* is used to indicate the uniform approach spray velocity far upstream of the cylinder, while \bar{U} represents the local tangential gas velocity on the upstream face of the cylinder just outside the boundary layer. The boundary layer analysis is based on the following assumptions which are valid for the Reynolds number range for incompressible gas flow in which forced convection is the dominant mode of heat transfer:

1. Spray transport properties are those of the continuous gas phase alone are constant, and liquid transport properties are constant.
2. Liquid and gas phase density are each constant.

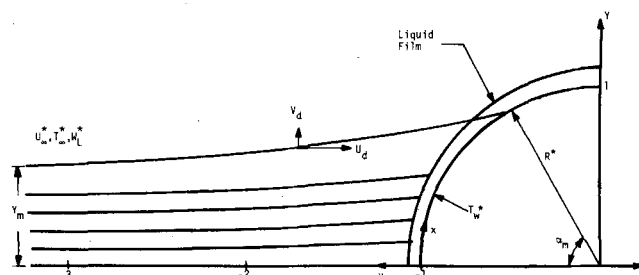


Figure 1. Spray flow trajectories: $K = 4$, $Re_s^2/K = 1000$.

TABLE 1. DRAG COEFFICIENT CONSTANTS

$A_0 = 1.01405502$	$A_1 = -2.37077754 \times 10^{-1}$
$A_2 = 3.84014924 \times 10^{-1}$	$A_3 = 6.83158450 \times 10^{-3}$
$A_4 = -4.5867258 \times 10^{-5}$	$A_5 = 8.12899339 \times 10^{-6}$
$A_6 = -6.9084339 \times 10^{-8}$	$A_7 = 2.295610 \times 10^{-10}$

3. Liquid drops are uniformly distributed throughout the gas and have the same velocity as the gas far upstream of the cylinder.

4. The gas is saturated with vapor at the upstream location.

5. The effects of surface tension, wave formation, viscous dissipation and gravity are negligible.

6. The gas phase flow field upstream of the cylinder may be determined from single-phase potential flow theory.

Drop motion in the gas flow field upstream of the cylinder is governed by the following conservation of momentum equations:

$$\frac{dU_d}{dX} = \frac{1}{U_d} \frac{1}{K} \frac{C_d Re}{24} (U_g - U_d) \quad (1)$$

$$\frac{dV_d}{dX} = \frac{1}{U_d} \frac{1}{K} \frac{C_d Re}{24} (V_g - V_d) \quad (2)$$

where the streamlines are given by

$$\frac{dY}{dX} = \frac{V_d}{U_d} \quad (3)$$

The boundary conditions on drop motion are

$$X \xrightarrow{\text{lim}} -\infty U_d(X, Y) = 1, X \xrightarrow{\text{lim}} -\infty V_d(X, Y) = 0 \quad (4)$$

corresponding to equality of drop and gas velocity far upstream of the cylinder. The potential flow velocity components for the gas are

$$U_g = 1 - \frac{X^2 - Y^2}{(X^2 + Y^2)^2}, V_g = -\frac{2XY}{(X^2 + Y^2)^2} \quad (5)$$

Experimental data on drag coefficient C_d and local Reynolds number Re have been tabulated by Bergrun (1947) as a relation between $C_d Re/24$ and Re . The following formula is obtained from a curve fit to this data, and the resulting C_d calculations are in agreement with data from Schlichting (1960) up to $Re = 10,000$. The values of the constants A_j are given in Table 1.

$$C_d Re/24 = A_0 + A_1 Re^{0.2} + A_2 Re^{0.5} + A_3 Re^{1.0} + A_4 Re^{1.7} + A_5 Re^{2.0} + A_6 Re^{2.3} + A_7 Re^{3.0} \quad (6)$$

Under the boundary layer assumption, the governing conservation equations are written for the liquid layer and spray layer in dimensionless form as follows. The stream function ψ is used, where $u = +\partial\psi/\partial y$, $v = -\partial\psi/\partial x$.

Liquid layer momentum

$$\frac{\partial\psi_L}{\partial y} \frac{\partial^2\psi_L}{\partial x\partial y} - \frac{\partial\psi_L}{\partial x} \frac{\partial^2\psi_L}{\partial y^2} = -\frac{1}{2\rho_L} \frac{dP}{dx} + \frac{\nu_L}{Re_\infty} \frac{\partial^3\psi_L}{\partial y^3} \quad (7)$$

Liquid layer energy

$$\frac{\partial\psi_L}{\partial y} \frac{\partial\theta_L}{\partial x} - \frac{\partial\psi_L}{\partial x} \frac{\partial\theta_L}{\partial y} = \frac{\nu_L}{Pr_L Re_\infty} \frac{\partial^2\theta_L}{\partial y^2} \quad (8)$$

Gas layer momentum

$$\frac{\partial\psi_g}{\partial y} \frac{\partial^2\psi_g}{\partial x\partial y} - \frac{\partial\psi_g}{\partial x} \frac{\partial^2\psi_g}{\partial y^2} = -\frac{1}{2} \frac{dP}{dx} + \frac{1}{Re_\infty} \frac{\partial^3\psi_g}{\partial y^3} \quad (9)$$

Gas layer energy

$$\frac{\partial\psi_g}{\partial y} \frac{\partial\theta_g}{\partial x} - \frac{\partial\psi_g}{\partial x} \frac{\partial\theta_g}{\partial y} = \frac{1}{Pr_g Re_\infty} \frac{\partial^2\theta_g}{\partial y^2} \quad (10)$$

Gas layer vapor species

$$\frac{\partial\psi_g}{\partial y} \frac{\partial N}{\partial x} - \frac{\partial\psi_g}{\partial x} \frac{\partial N}{\partial y} = \frac{1}{Sc Re_\infty} \frac{\partial^2 N}{\partial y^2} \quad (11)$$

The boundary conditions for these equations are

$$\frac{\partial\psi_L}{\partial y}(x, 0) = \frac{\partial\psi_L}{\partial x}(x, 0) = 0, \theta_L(x, 0) = 1,$$

$$y \xrightarrow{\text{lim}} \infty \frac{\partial\psi_g}{\partial y}(x, y) = \bar{U}(x), y \xrightarrow{\text{lim}} \infty N(x, y) = 1,$$

$$y \xrightarrow{\text{lim}} \infty \theta_g(x, y) = 0 \quad (12)$$

corresponding to zero velocity and constant temperature at the wall, and the local free stream velocity, temperature and vapor concentration which are distributed around the cylinder as the outer limiting conditions on the boundary layer.

At the interface separating the liquid layer and the gas layer, the boundary layer variables are related through interface conservation laws which provide the following interface conditions for solution of the governing differential equations in each layer and the determination of interface thickness.

Equality of tangential velocity

$$u_L = u_g \quad (13)$$

Equality of temperature

$$\theta_L = \theta_g \quad (14)$$

Conservation of total mass

$$\frac{W_{di}^* u_d^*}{\rho_\infty^* U_\infty^*} \frac{d\delta}{dx} + \frac{W_{di}^* v_d^*}{\rho_\infty^* U_\infty^*} + u_g \frac{d\delta}{dx} + \rho_L v_L = v_g + \rho_L u_L \frac{d\delta}{dx} \quad (15)$$

Conservation of mass of liquid and vapor

$$\frac{W_{di}^* u_d^*}{\rho_\infty^* U_\infty^*} \frac{d\delta}{dx} + \frac{W_{di}^* v_d^*}{\rho_\infty^* U_\infty^*} + \rho_L \left(v_L - u_L \frac{d\delta}{dx} \right) + \rho_g \left(u_g \frac{d\delta}{dx} - v_g \right) = -\frac{W_{v\infty}}{Sc Re_\infty} \frac{\partial N}{\partial y} \quad (16)$$

Conservation of thermal energy

$$\frac{W_{di}^* u_d^*}{\rho_\infty^* U_\infty^*} (\theta + Ev) \frac{d\delta}{dx} + \frac{W_{di}^* v_d^*}{\rho_\infty^* U_\infty^*} (\theta + Ev) + \rho_L v_L E_r - \rho_L u_L Ev \frac{d\delta}{dx} + \frac{\mu_L}{Re_\infty Pr_L} \frac{\partial\theta_L}{\partial y} = \frac{1}{Re_\infty Pr_g C_{pL}} \frac{\partial\theta_g}{\partial y} \quad (17)$$

Conservation of momentum in x direction

$$-\frac{\mu_L}{Re_\infty} \frac{\partial u_L}{\partial y} + \frac{1}{Re_\infty} \frac{\partial u_g}{\partial y} = \rho_L u_L^2 \frac{d\delta}{dx} - \rho_L u_L v_L - u_g^2 \frac{d\delta}{dx} + u_g v_g - \frac{W_{di}^* u_d^*}{\rho_\infty^* U_\infty^{*2}} \frac{d\delta}{dx} - \frac{W_{di}^* u_d^* v_d^*}{\rho_\infty^* U_\infty^{*2}} \quad (18)$$

Relation between vapor concentration and temperature

$$N = \frac{1 + \frac{\theta\pi_3}{Ev} + \pi_1 + \pi_2 \frac{\theta^2\pi_3^2}{Ev^2} + \pi_2\pi_1^2 + 2\pi_1\pi_2 \frac{\theta\pi_3}{Ev}}{1 + \pi_1 + \pi_1^2\pi_2 \frac{\theta\pi_3}{\pi_1 Ev} + 1} \quad (19)$$

The nondimensional parameters Re , Pr_L and Sc , which are common to single-phase flow, also govern the two-phase boundary layer. The additional parameter Ev is characteristic of two-phase flows and represents the ratio of latent heat to sensible heat within the boundary layer. The constants π_1 , π_2 and π_3 result from a quadratic approximation to the vapor pressure curve of the liquid and are given in the appendix.

In general, the drop concentration at the interface and the normal and tangential components of drop impingement veloc-

TABLE 2. DROP TRAJECTORY PARAMETERS

Re_0^2/K	K	α_m	Y_m	U_{d0}	U_{dm}	V_{dm}
0	0.4	0.626	0.154	0.195	0.45	0.485
	4	1.379	0.741	0.8175	1.039	0.194
	40	1.538	0.957	0.976	1.014	0.024
100	0.4	0.55	0.114	0.14	0.38	0.51
	4	1.291	0.68	0.7325	1.030	0.286
	40	1.504	0.928	0.948	1.022	0.06
1 000	0.4	0.416	0.08	0.1035	0.26	0.37
	4	1.147	0.56	0.65	0.98	0.35
	40	1.495	0.888	0.9215	1.032	0.097

ity are dependent on location on the upstream cylinder face. Consideration of mass concentration for the drops upstream of the cylinder gives the following nondimensional relation at the liquid interface:

$$W_{d\infty} \frac{dY_\infty}{dx} = \frac{W_{di}^* u_a^*}{\rho_\infty^* U_\infty^*} \frac{d\delta}{dx} + \frac{W_{di}^* v_a^*}{\rho_\infty^* U_\infty^*} \quad (20)$$

The relation between drop position in the free stream and the impingement angular position on the cylinder surface may be expressed by $Y_\infty = Y_m \sin(\pi/2 \alpha/\alpha_m)$ following Brun et al. (1953). The derivative of this expression is used in Equation (20).

Expressions for the horizontal and vertical velocity components for drop impingement on the cylinder surface are determined from the solution of Equations (1) to (5). The following relations are determined by curve fitting to that solution:

$$U_d = U_{d0} + (U_{dm} - U_{d0}) \left[1 - \cos \left(\frac{\pi}{2} \frac{\alpha}{\alpha_m} \right) \right] \quad (21)$$

$$V_d = V_{dm} \sin \left(\frac{\pi}{2} \frac{\alpha}{\alpha_m} \right) \quad (22)$$

The tangential component of drop impinging velocity is then obtained as

$$U_d = U_d \sin \alpha + V_d \cos \alpha \quad (23)$$

The expansion for the angle α in terms of x is immediately available. The variables α_m , Y_m , U_{d0} , U_{dm} and V_{dm} are determined from the solution of Equations (1) to (5) and are dependent on the values of K and Re_0^2/K as given in Table 2.

SOLUTION OF EQUATIONS

The velocity distribution in potential flow past a circular cylinder is given as follows by Schlichting (1960):

$$\bar{U}(x) = 2 \left[x - \frac{x^3}{3!} + \frac{x^5}{5!} - \frac{x^7}{7!} + \dots \right] \quad (24)$$

The pressure distribution on the upstream surface is given by

$$-\frac{1}{2\rho_g} \frac{dP}{dx} = \bar{U}(x) \frac{d\bar{U}(x)}{dx} = 4x - \frac{16}{3!} x^3 + \frac{64}{5!} x^5 - \frac{256}{7!} x^7 + \dots \quad (25)$$

The coordinate perturbation technique is used to reduce the governing partial differential equations into sets of ordinary differential equations with corresponding boundary conditions. The dependent variables are expanded as follows, where

$$\eta = y(2Re_\infty)^{1/2}$$

$$\psi_L(x, y) = \frac{1}{(2Re_\infty)^{1/2}} \left[2x f_1(\eta) - \frac{8}{3!} x^3 f_3(\eta) + \frac{12}{5!} x^5 f_5(\eta) - \frac{16}{7!} x^7 f_7(\eta) + \dots \right] \quad (26)$$

$$\psi_g(x, y) = \frac{1}{(2Re_\infty)^{1/2}} \left[2x g_1(\eta) - \frac{8}{3!} x^3 g_3(\eta) + \frac{12}{5!} x^5 g_5(\eta) \right]$$

$$- \frac{16}{7!} x^7 g_7(\eta) + \dots \quad (27)$$

$$\theta_L(x, y) = F_0(\eta) + F_2(\eta) \frac{x^2}{2!} + F_4(\eta) \frac{x^4}{4!} + F_6(\eta) \frac{x^6}{6!} + \dots \quad (28)$$

$$\theta_g(x, y) = G_0(\eta) + G_2(\eta) \frac{x^2}{2!} + G_4(\eta) \frac{x^4}{4!} + G_6(\eta) \frac{x^6}{6!} + \dots \quad (29)$$

$$N(x, y) = H_0(\eta) + H_2(\eta) \frac{x^2}{2!} + H_4(\eta) \frac{x^4}{4!} + H_6(\eta) \frac{x^6}{6!} + \dots \quad (30)$$

The liquid boundary layer thickness is a function only of x , given by

$$\delta(x) = (2Re_\infty)^{-1/2} \left[a_0 + a_2 \frac{x^2}{2!} + a_4 \frac{x^4}{4!} + a_6 \frac{x^6}{6!} + \dots \right] \quad (31)$$

At the interface, the variables f_n , F_n , g_n , G_n and H_n are functions only of x , since the liquid layer thickness is a function only of x . Each function then may be expanded in a Taylor series around the value at the stagnation point as given in the following example:

$$f_n(\eta_i) = f_n(\eta_{i0}) + f'_n(\eta_{i0}) \frac{\eta_i - \eta_{i0}}{1!} + f''_n(\eta_{i0}) \frac{(\eta_i - \eta_{i0})^2}{2!} + \dots \quad (32)$$

The other variables are expanded in a similar manner. The constant η_{i0} is determined from the liquid layer thickness at the stagnation point $a_0(2Re_\infty)^{-1/2}$.

When Equations (26) to (32) are substituted into the governing partial differential equations, interface relations and boundary conditions, and the coefficients of like powers of x are equated, sets of ordinary differential equations with corresponding boundary and interface conditions are obtained. Owing to the increasing length of the higher order equations, the first-order equations are listed here, and the second-, third- and fourth-order equations may be found from Lu (1972).

Differential equations:

$$f_1'^2 - f_1 f_1'' = \frac{1}{\rho_L} + \nu_L f_1''' \quad (33)$$

$$F_0' f_1 Pr_L + \nu_L F_0'' = 0 \quad (34)$$

$$g_1'^2 - g_1 g_1'' = 1 + g_1''' \quad (35)$$

$$G_0' g_1 Pr_g + G_0'' = 0 \quad (36)$$

$$H_0' g_1 Sc + H_0'' = 0 \quad (37)$$

Boundary conditions:

$$\eta = 0: f_1 = f_1' = 0, F_0 = 1 \quad (38)$$

$$\lim \eta \rightarrow \infty: g_1' = H_0 = 1, G_0 = 0 \quad (39)$$

$$\eta = \eta_{i0}: f_1' = g_1', F_0 = G_0 \quad (40)$$

$$g_1 = \rho_L f_1 - \frac{\beta}{2} \left(\frac{\pi}{2} \frac{Y_m}{\alpha_m} \right)$$

TABLE 3. GOVERNING PARAMETERS

Parameter	Value	Parameter	Value
μ_L	38.2	$W_{i\infty}$	0.0153
Pr_L	4.78	$C_{\mu L}$	4.15
Pr_g	0.708	π_1	-2.09
ρ_L	828.0	π_2	0.251
Sc	0.60	π_3	-4.12
Ev	34.8		

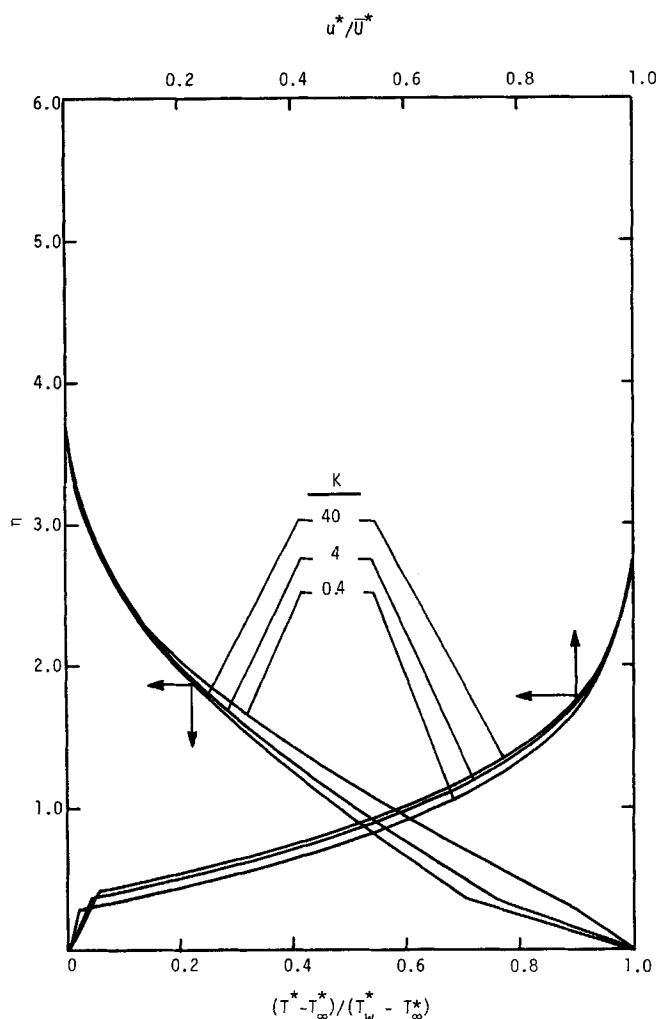


Figure 2. Velocity and temperature distributions: $\alpha^* = 0$, $\beta = 16$, $Re_0^2/K = 1000$.

$$g_1'' = \mu_L f_1' + \rho_L f_1' f_1 - g_1' g_1 - \frac{\beta}{4} \left(\frac{\pi}{2} \frac{Y_m}{\alpha_m} \right) \left(U_{d0} + \frac{\pi}{2} \frac{V_{dm}}{\alpha_m} \right)$$

$$G_0' = \frac{Pr_0 C_{PL}}{2} \left[\beta \left(\frac{\pi}{2} \frac{Y_m}{\alpha_m} \right) (F_0 + Ev) - 2\rho_L f_1 Ev + \frac{2\mu_L}{Pr_L} F_0' \right]$$

$$H_0 = \frac{1 + \frac{F_0 \pi_3}{Ev} + \pi_1 + \pi_2 \frac{F_0^2 \pi_3^2}{Ev^2} + \pi_2 \pi_1^2 + 2\pi_2 \pi_1 \frac{F_0 \pi_3}{Ev}}{\left[1 + \pi_1 + \pi_2 \pi_1^2 \right] \left[\frac{F_0 \pi_3}{Ev \pi_1} + 1 \right]}$$

$$H_0' = \frac{Sc}{W_{r\infty}} \left[\rho_L f_1 - W_{r\infty} H_0 g_1 - \frac{\beta}{2} \left(\frac{\pi}{2} \frac{Y_m}{\alpha_m} \right) \right]$$

The first-order set of equations corresponds to flow at the stagnation point, and the higher-order sets improve accuracy for higher values of x . The first four terms of each perturbation series are solved in the present analysis, since the higher-order terms become very small in determination of heat transfer, Lu (1972).

The two-point boundary value problems posed by the first four sets of equations were solved as initial value problems using fourth-order Runge-Kutta numerical integration. Wall condi-

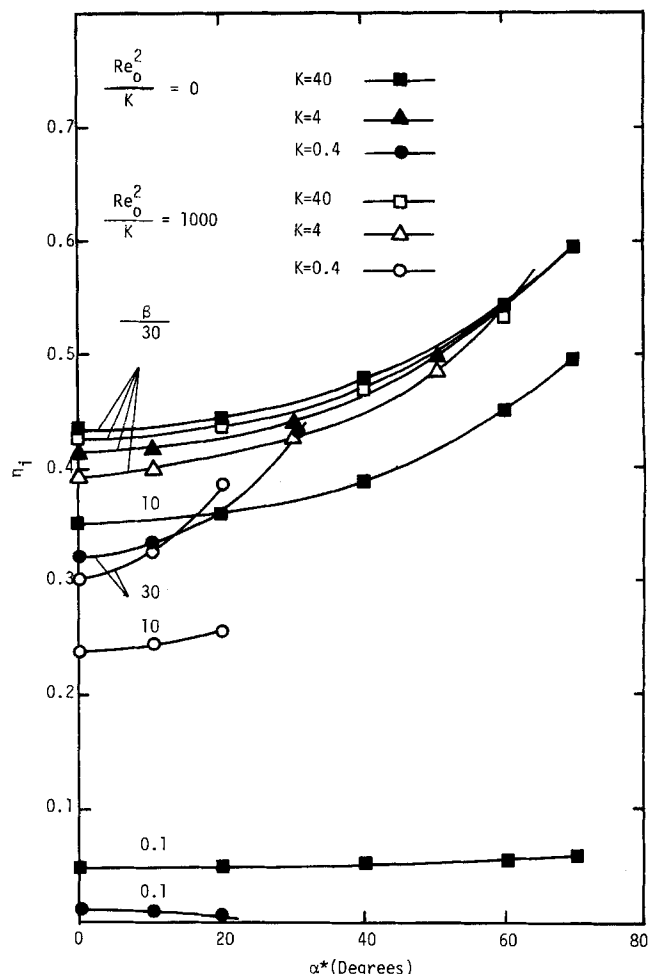


Figure 3. Liquid layer thickness.

tions and liquid layer thickness were assumed for the unknown values, and the equations were integrated until a check for the local conditions at the edge of the boundary layer was applied. A matrix Newton-Raphson routine was used to converge to the correct wall conditions and liquid film thickness.

The wall shear stress and heat flux are determined from the gradient of the temperature and velocity profiles at the wall, respectively:

$$\tau^* = -\mu_L^* \frac{\partial u_L^*(x,0)}{\partial y^*}, \quad q^* = -k_L^* \frac{\partial T_L^*(x,0)}{\partial y^*} \quad (41)$$

The local drag coefficient based on shear stress alone and Nusselt number are then calculated as

$$\frac{C_D(2Re_\infty)^{1/2}}{\mu_L} = -\frac{2\tau^*}{\rho_g^* U_\infty^{*2}} \frac{(2Re_\infty)^{1/2}}{\mu_L}$$

$$= 8xf_1''(0) - \frac{32}{3!} x^3 f_3''(0) + \frac{48}{5!} x^5 f_5''(0) - \frac{64}{7!} x^7 f_7''(0) + \dots \quad (42)$$

$$\frac{Nu}{(2Re_\infty)^{1/2}} = \frac{q^*}{(T_w^* - T_\infty^*)} \frac{2R^*}{k_L^*} \frac{1}{(2Re_\infty)^{1/2}}$$

$$= -2 \left[F_0'(0) + \frac{x^2}{2!} F_2'(0) + \frac{x^4}{4!} F_4'(0) + \frac{x^6}{6!} F_6'(0) + \dots \right] \quad (43)$$

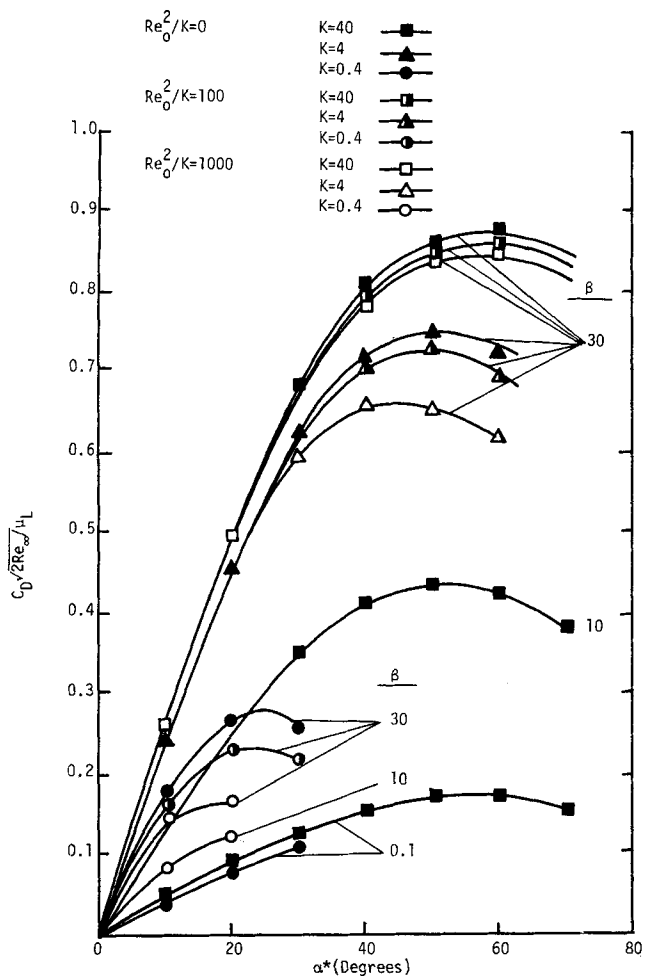


Figure 4. Drag coefficient.

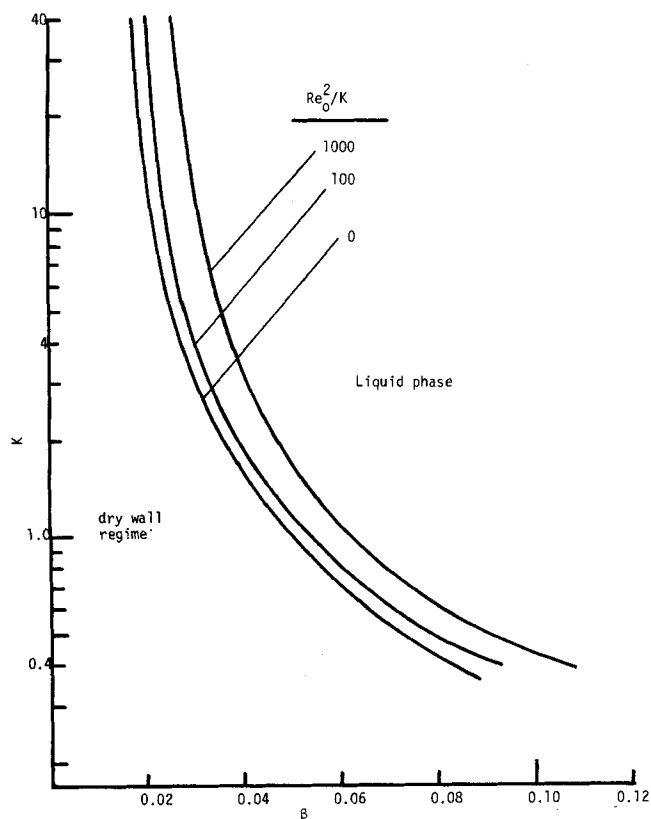


Figure 6. Dry out criteria.

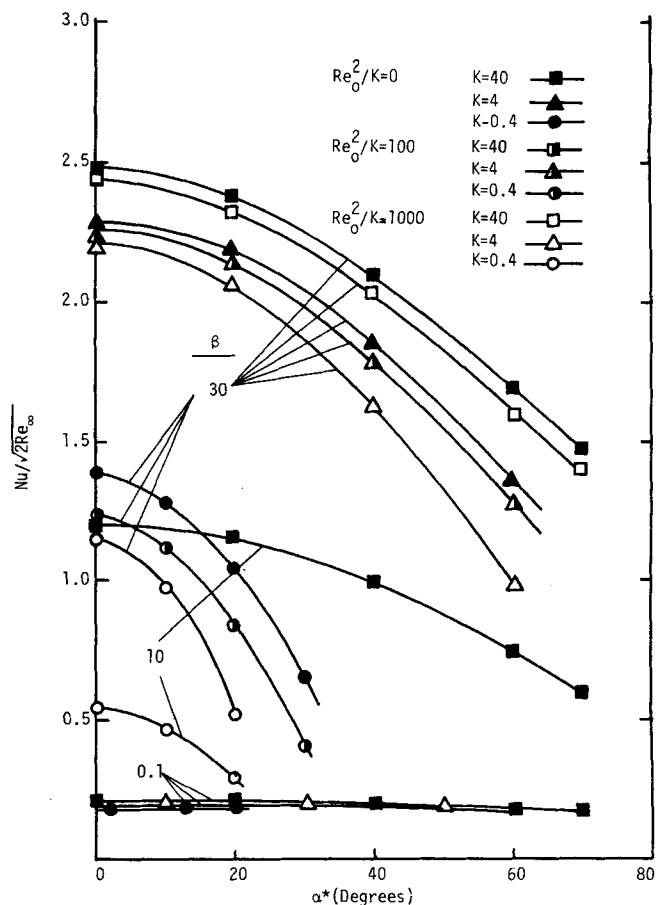


Figure 5. Nusselt number.

RESULTS AND DISCUSSION

The set of drop trajectories in Figure 1 shows the influence of drag forces from the gas, causing the drops to deviate from a straight trajectory and flow around the cylinder. The drops which impinge on the cylinder form the liquid film on the upstream face. The drops which originate from a location with $Y > Y_m$ never impinge on the cylinder and do not influence the boundary layer heat transfer. Drops impinge on the upstream surface for $\alpha \leq \alpha_m$, so the boundary layer results of this study apply only for this case.

Large values of the parameter K correspond to the motion of drops in an approximately straight trajectory. Low values of this

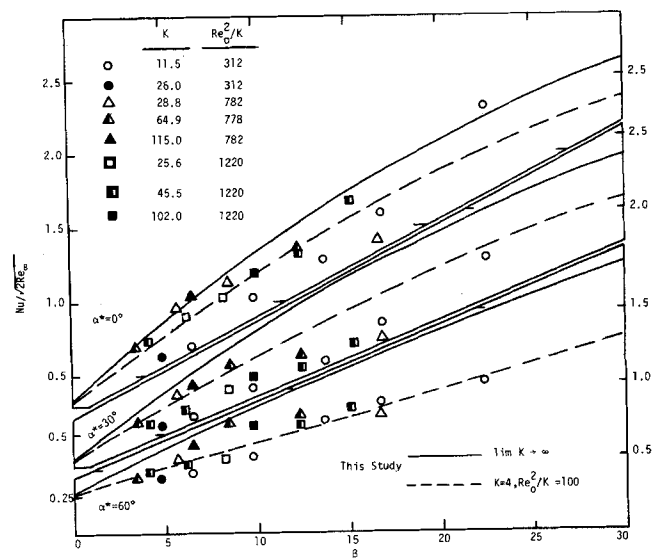


Figure 7. Experimental data.

TABLE 4. GOVERNING PARAMETERS FOR EXPERIMENT
(Hodgson et al., 1966)

$\mu_L = 34.84$	$W_{r\infty} = 0.0316$
$Pr_L = 4.34$	$C_{\mu L} = 4.16$
$Pr_g = 0.708$	$\pi_1 = -2.132$
$\rho_L = 874$	$\pi_2 = 0.251$
$Sc = 0.6$	$\pi_3 = -4.08$
$Ev = 34.6$	

parameter correspond to the case in which drops approximately follow the streamlines of the gas flow and move around the cylinder. Increasing cylinder diameter corresponds to increasing Re_0^2/K , which also tends to increase impingement on the cylinder.

Previous studies dealing with spray flow over a circular cylinder, Jain and Heyt (1972) and Heyt and Lu (1972), have indicated that the single parameter β has primary significance for correlating data in spray flow. Physically, this result indicates that drop flux entering the liquid layer in the direction normal to the cylinder is dominant. The nondimensional parameters given in Table 3 are typical of water-air spray under atmospheric conditions and are used for all results presented in Figures 1 to 6.

The tangential velocity and temperature profiles are shown in Figure 2 for selected values of K , keeping Re_0^2/K and β constant. The formation of liquid layer and gas layer is evident, as the corner in each profile marks the discontinuity slope between the two layers. An increase in the value of K tends to increase the thickness of the liquid layer owing to increased drop impingement on the upstream cylinder surface. The gradient in both the liquid tangential velocity and temperature also increase, resulting in increased surface shear stress and heat transfer.

The variation of the liquid film thickness with angular position on the upstream cylinder face and the parameters affecting drop trajectory is shown in Figure 3. For a given value of β , the film thickness is seen to increase for increasing values of K and decreasing values of Re_0^2/K . The maximum angle indicated by each of the interface thickness curves corresponds to the maximum angle of drop impingement on the cylinder surface and thus the maximum angle for which the present theory is applicable. For the low values of K , it is evident that the drops impinge only for small values of α . For $\beta = 10$, only the maximum and minimum liquid layer thickness curves are shown. For $\beta = 0.1$, drops impinge on an appreciable amount of the cylinder only for the lower values of Re_0^2/K .

The variation with angular position of the local drag coefficient based upon wall shear and the local Nusselt number are shown in Figures 4 and 5, respectively. For a given value of β , the increase in wall shear and heat transfer with increasing K reflects the increase in liquid layer thickness. At the low values of β , the effects of drop trajectory have only a small effect on shear and heat transfer, since the values for the two-phase flow approach those for single-phase flow.

At low values of β , the liquid film thickness is found to decrease with increasing α . The entire upstream face of the cylinder is thus dry when the liquid film thickness has vanished at the stagnation point. The influence of drop trajectory on the criteria for wall dry-out is shown in Figure 6. The region above and to the right of each curve corresponds to the liquid film regime, and the region below and to the left corresponds to the dry wall regime. At low values of K , corresponding to drops which tend to flow around the cylinder following the gas, the liquid layer dries out at higher liquid content. Increasing the parameter Re_0^2/K also increases the value of β for which the film vanishes.

Experimental data reported by Hodgson et al. (1966) are shown in Figure 7 in comparison to theoretical predictions of the present study. The set of parameters matching the experimental conditions is given in Table 4. Whereas theory based on straight drop trajectory tends to overestimate the heat transfer at large values of β , the theory including trajectory curvature is in agreement with the trend of the data.

APPENDIX

The nondimensional vapor concentration at the interface between the liquid layer and the outer spray boundary layer is obtained by first expressing the vapor pressure of the liquid as an approximate quadratic function of temperature:

$$P_i^* = C_1^* + C_2^* T^* + C_3^* T^{*2} \quad (A1)$$

Calculation of the concentration ratio then gives

$$N = \frac{W_r}{W_{r\infty}} \frac{\rho_i^*}{\rho_{r\infty}} = \frac{P_i^* T_{\infty}^*}{P_{r\infty}^* T^*} \quad (A2)$$

Substitution of Equation (A1) into Equation (A2) with use of dimensionless variables gives Equation (19).

NOTATION

Symbols with the superscript (*) are dimensional quantities, all others are dimensionless.

a_n	= constants in the expansion of liquid layer thickness
C_1^*, C_2^*, C_3^*	= constants for vapor pressure curve of the liquid
C_d	= drag coefficient of liquid drops in gas phase
C_{Dl}	= local drag coefficient, $2\tau^*/\rho_g^* U_{\infty}^{*2}$
C_p	= specific heat, C_p^*/C_{pg}^*
D_{vg}^*	= mass diffusivity of vapor in noncondensable gas
Ev	= evaporation number, $\lambda^*/(C_{pg}^* (T_w^* - T_{\infty}^*))$
$f_n(\eta)$	= liquid layer velocity variables
$F_n(\eta)$	= liquid layer temperature variables
$g_n(\eta)$	= gas layer velocity variables
$G_n(\eta)$	= gas layer temperature variables
h^*	= local wall heat transfer coefficient
$H_n(\eta)$	= gas layer vapor concentration variables
K	= inertia parameter, $(2/9) (\rho_d r^2 Re_{\infty})$
k^*	= thermal conductivity
N	= vapor concentration ratio, $W_r/W_{r\infty}$
Nu	= local wall Nusselt number, $2 h^* R^*/k_L^*$
P	= pressure, $P^*/\rho_g^* U_{\infty}^{*2}/2$
Pr	= Prandtl number, $\mu^* C_p^*/k^*$
q^*	= local heat flux at the wall
R^*	= radius of cylinder
r	= radius of liquid drop, r^*/R^*
Re	= local Reynolds number with respect to drop, $2r^* \rho_g^* [(U_g^* - U_d^*)^2 + (V_g^* - V_d^*)^2]^{1/2} / \mu_g^*$
Re_0	= free stream Reynolds number with respect to drop, $2r^* \rho_g^* U_{\infty}^* / \mu_g^*$
Re_{∞}	= free stream Reynolds number with respect to cylinder, $R^* \rho_g^* U_{\infty}^* / \mu_g^*$
Sc	= Schmidt number, ν_g^*/D_{vg}^*
T^*	= temperature
u	= local x direction velocity, u^*/U_{∞}^*
U	= local X direction velocity, U^*/U_{∞}^*
U_{∞}^*	= reference velocity far removed from cylinder
\bar{U}	= potential flow velocity at liquid boundary layer edge, \bar{U}^*/U_{∞}^*
v	= local y direction velocity, v^*/U_{∞}^*
V	= local Y direction velocity, V^*/U_{∞}^*
W	= mass concentration, W^*/ρ_g^*
x	= coordinate tangential to cylinder surface, x^*/R^*
X	= coordinate parallel to free stream velocity, X^*/R^*
y	= coordinate normal to cylinder surface, y^*/R^*
Y	= coordinate normal to free stream velocity, Y^*/R^*

Greek Letters

α^*	= angle giving location on cylinder surface
β	= $W_{d\infty} (2Re_{\infty})^{1/2}$
δ	= liquid boundary layer thickness, δ^*/R^*
η	= $y/(2Re_{\infty})^{1/2}$
θ	= temperature, $(T^* - T_{\infty}^*)/(T_w^* - T_{\infty}^*)$
λ^*	= enthalpy of vaporization of liquid
ν	= kinematic viscosity, ν^*/ν_g^*

μ = absolute viscosity, μ^*/μ_{∞}^*
 π_1 = $T_{\infty}^* C_2^*/C_1^*$
 π_2 = $C_1^* C_3^*/C_2^{*2}$
 π_3 = $(C_2^*/C_1^*) (\lambda^*/C_{PL}^*)$
 ρ = density, ρ^*/ρ_{∞}^*
 τ^* = local shear stress at the wall
 ψ = stream function

Subscripts

d = liquid drop
 g = gas properties
 i = interface at liquid/gas boundary layers
 L = liquid properties
 m = maximum value for impingement on surface
 0 = stagnation point
 w = condition at wall
 ∞ = free stream conditions

Superscripts

$'$ = derivative with respect to the independent variable
 $^{\circ}$ = degrees

LITERATURE CITED

- Acrivos, A., J. E. Ahearn and A. R. Nagy, "Research Investigation of Two Component Heat Transfer," *ARL Rept. 64-116* (1964).
 Bergrun, N. R., "A Method for Numerically Calculating the Area and Distribution of Water Impingement on the Leading Edge of an Airfoil in a Cloud," *NACA TN 1397* (1947).
 Brun, R. J., and H. W. Mergler, "Impingement of Water Droplets on a Cylinder in an Incompressible Flow Field and Evaluation of Rotating Multicylinder Method for Measurement of Droplet-Size Distribution, Volume-Median Droplet Size, and Liquid-Water Content in Clouds," *NACA TN 2904* (1953).
 Elperin, I. T., "Heat Transfer of Two-Phase Flow with a Bundle of Tubes," *Inzhenero-Fizicheskii Zhurnal*, 4, 30 (1961).
 Goldstein, M. E., W. J. Yang and J. A. Clark, "Boundary Layer Analysis of Two Phase Flow over an Oscillating Flat Plate," *AIAA J.*, 5, 43 (1967).
 ———, "Momentum and Heat Transfer in Laminar Flow of Gas with Liquid Droplet Suspension over a Circular Cylinder," *J. Heat Transfer*, 89, 185 (1967).
 Goodman, W., "The Evaporative Condenser," *Heating, Piping, and Air Conditioning*, 10, 165, 255, 327 (1938).
 Heyt, J. W., and P. W. Larsen, "Heat Transfer to Binary Mist Flow," *International J. Heat and Mass Transfer*, 14, 1395 (1971).
 Heyt, J. W., and C. C. Lu, "Heat Transfer to Binary Spray Flow with Applied Heat Flux," Southeastern Seminar on Thermal Sciences, Vanderbilt Univ., Nashville, Tenn. (Mar., 1972).
 Hodgson, J. W., R. T. Saterbak and J. E. Sunderland, "An Experimental Investigation of Heat Transfer from a Spray Cooled Isothermal Cylinder," *J. Heat Transfer*, 90, 457 (1966).
 Hodgson, J. W., and J. E. Sunderland, "Heat Transfer from a Spray Cooled Isothermal Cylinder," *Ind. Eng. Chem. Fundamentals*, 7, 567 (1968).
 Hoelscher, J. F., Study of Heat Transfer from a Heated Cylinder in Two Phase, Water-Air Flow," M.S. thesis, School of Engineering, Air University, United States Air Force (1965).
 Jain, S. C., and J. W. Heyt, "Evaporation and Liquid Film Dry-Out in Binary Spray Flow," 1972 National Heat Transfer Conference, Denver, Colo. (Aug., 1972).
 James, B. E., "A Study of Heat Transfer in Unit Refrigerant Condensers Which Use Evaporative Cooling," *J. ASRE*, 169 (1937).
 Lu, C. C., "Flow Regime Transition in Binary Spray Flow: Influence of Drop Trajectory," Ph.D. thesis, Univ. Tex., Austin (1972).
 Mednick, R. L., and C. P. Colver, "Heat Transfer from a Cylinder in an Air-Water Spray Flow Stream," *AIChE J.*, 15, 357 (1969).
 Schlichting, H., *Boundary Layer Theory*, 4 ed., Translated by J. Kestin, McGraw-Hill, New York (1960).
 Smith, J. E., "Heat Transfer Studies of Water-Spray Flows," *ARL Rept.*, 66 (1966).
 Takahara, E. W., "Experimental Study of Heat Transfer from a Heated Circular Cylinder in Two-Phase, Water-Air Flow," M.S. thesis, School of Engineering, Air University, United States Air Force (1966).
 Thomsen, E. G., "Heat Transfer in an Evaporative Condenser," *Refrigeration Engineering*, 425 (1946).
 Thomas, W. C., "Heat Transfer from a Wall Cooled by a Liquid Spray," Ph.D. thesis, Georgia Inst. Technol., Atlanta (1967).
 Tifford, A. N., "Exploratory Investigation of Laminar Boundary Layer Heat Transfer Characteristics of Gas-Liquid Spray Systems," *ARL Rept.*, 64-136 (1964).
 Wile, D. D., "Evaporative Condenser Performance Factors," *Refrigeration Engineering*, 55 (1950).
 Yeh, H. C., and W. J. Yang, "Stagnation Point Forced Convection in Two Phase Flow," *AIAA J.*, 5, 1182 (1967).
 Manuscript received June 4, 1979; revision received October 25, and accepted November 7, 1979.

The Calculation of Critical Points

Gibb's classical theory of critical points leads to two simultaneous, nonlinear equations in the intensive variables of the critical phase. In this paper is presented a new procedure for evaluating the functions which appear in these nonlinear equations. The new procedure simplifies and permits the speeding up of the computation of critical points in multicomponent mixtures.

Computations have been performed for critical points in binary and multicomponent mixtures described by the SRK equation. The methods developed will be equally applicable to other two-constant equations of state. The equations to be solved are organized as two equations in the unknown critical temperature and specific volume for a mixture of known composition. One of the two equations, the determinant which establishes the stability limit for the mixture, is shown to be satisfied by more than one volume at a given temperature and by several temperatures at a given volume. A technique is proposed to assure that the correct temperature, volume solution can be found for this equation. For critical points in ordinary gas-liquid systems, an overall computational procedure is suggested in which it proves to be unnecessary to provide initial guesses for either the temperature or the volume.

Application has also been made to several systems with high density (liquid-liquid) critical points.

This paper deals with the calculation of critical points in multicomponent mixtures in which all fluid phases are described by an equation of state. Various equations of state are

SCOPE

widely used to correlate phase equilibrium in mixtures, particularly mixtures of hydrocarbons. Among these are two constant equations proposed by Wilson (1969), Soave (1972) and Peng and Robinson (1976). Phase equilibrium computation

ROBERT A. HEIDEMANN

and

AHMED M. KHALIL

Department of Chemical Engineering
The University of Calgary
Calgary, Alberta T2N 1N4 Canada